Efficient optical excitation transfer in layered quantum dot nanostructures networked via optical near-field interactions

Makoto Naruse,[1,2] Erich Runge,[3] Kiyoshi Kobayashi,[4] and Motoichi Ohtsu[2]
[1]*National Institute of Information and Communications Technology, 4-2-1 Nukui-kita, Koganei, Tokyo 184-8795, Japan*
[2]*Department of Electrical Engineering and Information Systems and Nanophotonics Research Center, School of Engineering, The University of Tokyo, 2-11-16 Yayoi, Bunkyo-ku, Tokyo 113-8656, Japan*
[3]*Institute of Physics and Institute of Micro- and Nanotechnologies, Ilmenau University of Technology, 98684 Ilmenau, Germany*
[4]*Interdisciplinary Graduate School of Medicine and Engineering, University of Yamanashi, Kofu, Yamanashi 400-8511, Japan*
(Received 11 February 2010; revised manuscript received 17 August 2010; published 9 September 2010)

We investigated the efficient optical excitation transfer in layered quantum dot structures by introducing a network of optical near-field interactions. With a density-matrix-based formalization of interdot near-field interactions, our theoretical approach allows systematic analysis of layered CdTe quantum dot systems, revealing dominant factors contributing to the efficient optical excitation transfer and demonstrating good agreement with previous experimental observations. We also show that the efficiency of optical excitation transfer could be further improved by optimizing the interaction network.

DOI: 10.1103/PhysRevB.82.125417 PACS number(s): 78.67.Bf, 74.25.Gz, 73.63.Kv

I. INTRODUCTION

Optical near-field interactions on the nanometer scale have been studied intensively both theoretically and experimentally because of their potential impact in a wide range of applications. One of their unique enabling functions is optical excitation transfer between nanoscale matter, such as semiconductor quantum dots (QDs), via optical near-field interactions.[1] This offers various applications, including subwavelength-scale optical devices beyond the diffraction limit of light,[2–5] light harvesting systems,[6–9] nanofabrication,[10] and many others. Experimental materials exploiting optical near-field interactions have been seeing rapid progress, such as randomly diffused quantum dots,[11–14] geometry-controlled quantum dot arrangements,[15,16] ZnO nanorods,[17] and others. Theoretical fundamentals have also been built, such as in the dressed photon model,[1] which explains the possibility of optical transitions between conventionally electric dipole forbidden energy levels, thanks to the localized nature of a photon dressed by material excitations in its vicinity.[18]

One of the most interesting consequences of optical excitation transfer is energy concentration to larger quantum dots from smaller ones via optical near-field interactions. Those have been observed in some materials, most notably CuCl,[3,6] CdSe,[14,15] CdTe,[19,20] and InAs quantum dots.[21] In Refs. 19 and 20, the Feldmann group experimentally demonstrated *superefficient* energy concentration, where the radiation from layered graded-size CdTe quantum dots exhibits a signal nearly four times larger than that from structures composed of uniform-size quantum dots, which has been called *exciton recycling*[19] or *superefficient exciton funneling*.[20]

In the literature, dipole-dipole interactions such as Förster resonant energy transfer are typically used in explaining energy transfer from smaller QDs to larger ones.[15,22] However, it should be noted that such point-dipole-based modeling does not allow optical transitions to dipole-forbidden energy sublevels, which is often the case with the experimental conditions of two closely located QDs of slightly different size (rigorously, with a size ratio of 1.45 in the case of spherical QDs, as discussed in Sec. II). Also, recent experimental observations in light harvesting antenna indicate the inaccuracy of dipole-based modeling.[9,23] On the other hand, as mentioned already above, the localized nature of optical near fields frees us from conventional optical selection rules, meaning that optical excitation could excite QDs to energy levels that are conventionally electric dipole forbidden.[1,4] This has been demonstrated experimentally and validated theoretically in, e.g., logic devices and systems,[24] and energy concentration applications.[3,6]

In this paper, we analyze the superefficient energy concentration in layered QD systems like those experimentally reported in Refs. 19 and 20 within the theoretical framework of optical near-field interactions. We formulate an interaction network among layered nanostructures whereby the dynamics of the structure-dependent optical excitation transfer involving electric dipole forbidden energy levels is systematically analyzed based on a density-matrix formalism. We demonstrate that the increase in the radiation from the graded-size quantum dot system shows good agreement between the experiment and theory.

This paper is organized as follows. In Sec. II, we first review the experimental observations in layered CdTe quantum dot nanostructures reported so far and describe theoretical elements of optical excitation transfer via optical near-field interactions. In Sec. III, we demonstrate the modeling of the interaction networks in the layered quantum dot systems. In Sec. IV, we quantitatively analyze the structure-dependent optical excitation transfer, including its agreement with the experiments. Also, we demonstrate another system showing further improved efficiency in optical excitation transfer. Section V concludes the paper.

II. REVIEW OF EXPERIMENTAL AND THEORETICAL ELEMENTS OF OPTICAL NEAR-FIELD INTERACTIONS

First we briefly summarize the experimental observations reported in Ref. 19 that shows optical excitation transfer in

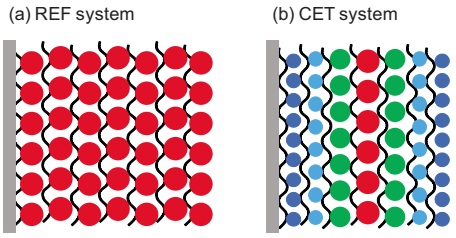

FIG. 1. (Color online) (a) Layered quantum dot system consisting of uniform-sized elements, called the REF system. (b) Layered quantum dot system consisting of four different, graded-sized elements, called the CET system.

two kinds of representative layered nanostructures. One kind is a system consisting of quantum dots of the same size, as schematically shown in Fig. 1(a), called a reference (REF) system. It consists of seven layers of 3.5-nm-diameter CdTe quantum dots. The other system, called a cascaded energy transfer (CET) system, shown in Fig. 1(b), also has a seven-layer structure, but the diameters are stepwise increasing in the first four layers (1.7, 2.5, 3.2, and 3.5 nm) and stepwise decreasing in the subsequent three layers (3.2, 2.5, and 1.7 nm). These REF and CET systems were synthesized using layer-by-layer assembly methods.[25,26]

With optical excitation at a wavelength of 350 nm, the CET system exhibits nearly four times larger photoluminescence than the REF system at emission wavelengths around 612 nm, which corresponds to the radiation from the 3.5-nm-diameter CdTe QDs.[19] Note that there is only one layer of 3.5-nm-diameter QDs in the CET system, whereas the REF system has seven layers of those QDs. Note that the experimental quantum yield of the REF system is very low, on the order of 2%, compared with a quantum yield of about 20% for isolated dots. The authors of Refs. 19 and 20 interpret their findings consistently in terms of nonradiative trap states and exciton recycling from the trap states of larger dots into QD states of smaller dots. It has been reported that these trap states are actually Te-related hole traps on the surface of the CdTe QDs.[27] In this paper, we call QDs having trap states *dark* dots.

In this section, we describe elements of the theoretical framework, which will be later applied in the analysis of the REF and CET systems in Sec. III. The present paper transfers the concept of layered CET systems to layered systems of QDs, such as those studied in Refs. 2 and 14 where excitation transfer via optical near-field interactions takes place between the ground states of smaller dots QD_S (radius R_S) and the first excited states of larger dots QD_L (radius R_L). The condition that these energy levels are in resonance can, for spherical QDs, be discussed using the simple, but widely used estimation of Brus[28] for the energy eigenvalues of QD states specified by the orbital angular momentum quantum number l and the magnetic quantum number m,[29]

$$E_{(n,l)} = E_g + \frac{\hbar^2 \alpha_{nl}^2}{2R^2}\left(\frac{1}{m_e} + \frac{1}{m_h}\right) - 1.8\frac{e^2}{\varepsilon R}. \quad (1)$$

Here, E_g is the band-gap energy of the bulk semiconductor, $m_e(m_h)$ is the effective mass of the electron (hole), ε is the dielectric constant, and α_{nl} are determined from the boundary conditions, for example, $\alpha_{n0}=n\pi$, $\alpha_{11}=4.49$.

According to Eq. (1), there exists a resonance between the level of quantum number (1,0) of QD_S and that of quantum number (1,1) of QD_L when the size ratio R_L/R_S is appropriately configured. Based on the material parameters for CdTe QDs (Ref. 30) used in the experiment described above, whose radii range from around 1–4 nm, such a resonance occurs when $R_L/R_S \sim 1.45$ is satisfied. The nominal ratio of the diameters of adjacent CdTe QDs in the experimental CET system does not exactly satisfy this condition. However, it is known that QD sizes could typically tolerate a $\pm 10\%$ deviation from the optimal condition,[31] which includes the experimental combinations of the diameters of the QDs used.

It should be noted that optical transitions to the (1,1) level in QD_L are prohibited in conventional optical selection rules; only transitions to states specified by $l=m=0$ are allowed, where l and m are the orbital angular momentum quantum number and magnetic quantum number, respectively.[29] However, when those two QDs are closely located, thanks to the large spatial inhomogeneity of the localized optical near fields at the surface of nanoscale material, an optical transition that violates conventional optical selection rules is permitted.[1] Therefore, an exciton in the (1,0) level in QD_S could be transferred to the (1,1) level in QD_L. In QD_L, due to the sublevel energy relaxation, which is faster than the near-field interaction, the exciton relaxes to the (1,0) level. Therefore, unidirectional optical excitation transfers from QD_S to QD_L is accomplished.

III. NETWORK OF OPTICAL NEAR-FIELD INTERACTIONS IN LAYERED QUANTUM DOTS

A. Analysis of the REF system

1. Modeling of the REF system

We now consider optical excitation transfer in the REF and CET systems introduced in Sec. II with a network of interactions between QDs via optical near fields. First we consider modeling of the REF system. As shown in Fig. 2(a), we represent the REF system as a 5-row $\times$ 7-column system composed of the same-sized QDs and assume that only one QD in the system yields output radiation, whereas all of the others are dark. That is, the concentration of bright QD is $1/(5\times 7) \sim 2.9\%$, which is comparable to the experimental value of about 2% luminescence yield. Each of the quantum dots is identified by the notation QD_{S_i}, where the suffixes S and i, respectively, specify its horizontal position $S=\{A,B,C,D,E,F,G\}$ and vertical position $i=\{-2,-1,0,1,2\}$. We suppose that those QDs have two energy levels: the (1,0)-energy level in QD_{S_i} denoted by $S_i^{(1,0)}$ and the (1,1) level denoted by $S_i^{(1,1)}$. The sublevel relaxation constant from $S_i^{(1,1)}$ to $S_i^{(1,0)}$ is given by Γ_{S_i}, which is faster than the radiative or nonradiative relaxation constant from $S_i^{(1,0)}$, denoted by γ_{S_i}.

We assume interdot interactions in the (1,1) level as follows. The interactions between horizontally adjacent quantum dots are denoted by $U_{S_iT_i}$, where the suffixes are given

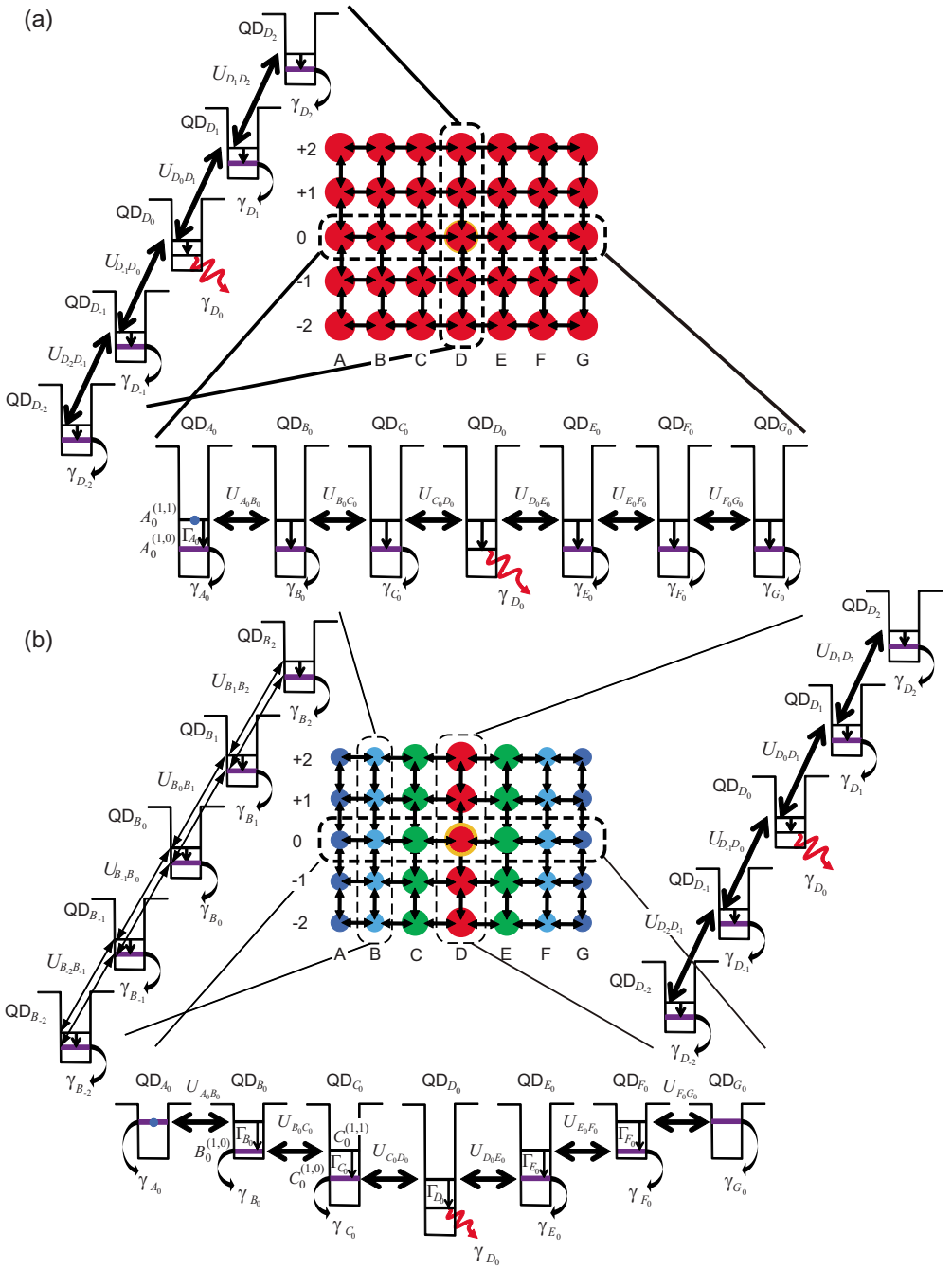

FIG. 2. (Color online) Theoretical modeling of (a) the REF system and (b) the CET system. The radiative relaxation from the center QD, denoted by QD_{D_0}, contributes to the output.

by $(S,T)=\{(A,B),(B,C),(C,D),(D,E),(E,F),(F,G)\}$ and $i=\{-2,\ldots,2\}$. At the bottom of Fig. 2(a), horizontal interactions among QDs located in row $i=0$ are schematically indicated. Also, the interactions between vertically adjacent quantum dots are given by $U_{S_iS_{i+1}}$, where $S=\{A,\ldots,G\}$ and $i=\{-2,-1,0,1\}$. The left-hand side of Fig. 2(a) schematically shows the array of QDs in column D.

Now, the interaction Hamiltonian regarding one-exciton states where an exciton exists at one of the energy levels of $S_i^{(1,1)}$ is given by submatrices H_i and $H_{i,j}$,

$$H_{\text{int}}^{(1,1)}=\begin{pmatrix} H_2 & H_{1,2} & O & O & O \\ H_{1,2} & H_1 & H_{0,1} & O & O \\ O & H_{0,1} & H_0 & H_{-1,0} & O \\ O & O & H_{-1,0} & H_{-1} & H_{-2,1} \\ O & O & O & H_{-2,1} & H_{-2} \end{pmatrix}, \quad (2)$$

where O represents an empty matrix. The diagonal elements in Eq. (2) specify horizontal interactions given by

$$H_i = \hbar \begin{pmatrix} 0 & U_{A_iB_i} & 0 & 0 & 0 & 0 & 0 \\ U_{A_iB_i} & 0 & U_{B_iC_i} & 0 & 0 & 0 & 0 \\ 0 & U_{B_iC_i} & 0 & U_{C_iD_i} & 0 & 0 & 0 \\ 0 & 0 & U_{C_iD_i} & 0 & U_{D_iE_i} & 0 & 0 \\ 0 & 0 & 0 & U_{D_iE_i} & 0 & U_{E_iF_i} & 0 \\ 0 & 0 & 0 & 0 & U_{E_iF_i} & 0 & U_{F_iG_i} \\ 0 & 0 & 0 & 0 & 0 & U_{F_iG_i} & 0 \end{pmatrix}, \tag{3}$$

where $i=\{-2,\ldots,2\}$ and $\hbar$ is Planck's constant divided by 2π. The nondiagonal elements in Eq. (2) describe the vertical interactions in the system, given by

$$H_{i,j} = \hbar \, \mathrm{diag}(U_{A_iA_j}, U_{B_iB_j}, U_{C_iC_j}, U_{D_iD_j}, U_{E_iE_j}, U_{F_iF_j}, U_{G_iG_j}), \tag{4}$$

where $(i,j)=\{(-2,-1),(-1,0),(0,1),(1,2)\}$. The sublevel relaxation from the energy levels of $S_i^{(1,1)}$ is described by a diagonal matrix $N_\Gamma^{(1,1)}$ whose diagonal elements are given by Γ_{S_i}. Letting $\rho^{(1,1)}(t)$ be the density matrix corresponding to the Hamiltonian introduced above and $H^{(0)}$ be the unperturbed Hamiltonian, the master equation for the system is given by[32]

$$\frac{d\rho^{(1,1)}(t)}{dt} = -\frac{i}{\hbar}[(H^{(0)} + H_{\mathrm{int}}^{(1,1)}), \rho^{(1,1)}(t)] - N_\Gamma^{(1,1)}\rho^{(1,1)}(t) - \rho(t)^{(1,1)}N_\Gamma^{(1,1)}. \tag{5}$$

The lower level in QD_{S_i}, namely, the (1,0) level denoted by $S_i^{(1,0)}$, could be filled via the sublevel relaxation denoted by Γ_{S_i} from $S_i^{(1,1)}$. The relaxation constants from $S_i^{(1,0)}$ are given by a diagonal matrix $N_\Gamma^{(1,0)}$ whose diagonal elements are given by γ_{S_i}.

Now, remember that only one QD in the system is bright and all the rest are dark. That is, most of the energy levels of $S_i^{(1,0)}$ should be treated as trap states. In representing those trap states in the REF system, we assume that there are no interactions between QDs among the energy levels of $S_i^{(1,0)}$. Letting $\rho^{(1,0)}(t)$ be the density matrix corresponding to the energy level of $S_i^{(1,0)}$, the master equation for the system is given by

$$\frac{d\rho^{(1,0)}(t)}{dt} = -\frac{i}{\hbar}[H_0, \rho^{(1,0)}(t)] - N_\Gamma^{(1,0)}\rho^{(1,0)}(t) - \rho^{(1,0)}(t)N_\Gamma^{(1,0)} + P_\Gamma[\rho^{(1,1)}(t)], \tag{6}$$

where P_Γ represents the relaxations from the energy levels of $S_i^{(1,1)}$.

2. Numerical evaluation of the REF system

In the numerical calculation, we assume that the horizontal and vertical interactions are equal; namely, we assume $U_{S_iT_i}^{-1} = U_{S_kS_{k+1}}^{-1} = 100$ ps. The radiation lifetime of the bright CdTe quantum dot is assumed to be 2 ns. The sublevel relaxation constants in QD_{S_i} are given by $\Gamma_{S_i}^{-1} = 10$ ps. We consider that QD_{D_0}, located in the center, is a bright one whose population regarding the (1,0) level gives an output signal, whereas all the other dots are dark ones whose (1,0)-level populations do not contribute to the output. Also, we regard the nonradiative relaxation time $\gamma_{S_i}^{-1} = 40$ ns $(S_i \neq D_0)$ from the (1,0) level of QD_{S_i} to be 20 times larger than the radiative relaxation time $\gamma_{D_0}^{-1} = 2$ ns. In experiments, the interdot interaction time between CdTe quantum dots has been reported to be 254 ps, and the possibility of 100 ps was discussed in Ref. 26; we investigate the interaction-time dependence later in Sec. IV. The radiation lifetime of CdTe QDs can range from hundreds of picoseconds up to hundreds of nanoseconds.[33] In this paper, as stated above, we set the radiation lifetime as $\gamma_{D_0}^{-1} = 2$ ns in agreement with the experimental findings in Ref. 34.

Then we assume that there is an initial exciton in either one of the (1,1) levels of the QDs in the system. Here, since the (1,1) level is an electric dipole forbidden energy level for propagating light, such an initial state is physically unreasonable. However, since the primary interest in this paper is to highlight the effects of interdot optical excitation transfer involving electric dipole forbidden energy levels, which play a critical role in the CET system described below, we assume such an initial condition, so that the input exciton could have the possibility of interacting with the adjacent dots.

Finally, by solving quantum master equations given by Eqs. (5) and (6), the time evolution of the (1,0) level of QD_{D_0} with initial excitation at the (1,1) level of QD_{S_i} is obtained, which is denoted by $\rho_{D_0}(t;S_i)$. For example, Fig. 3(a) dem-

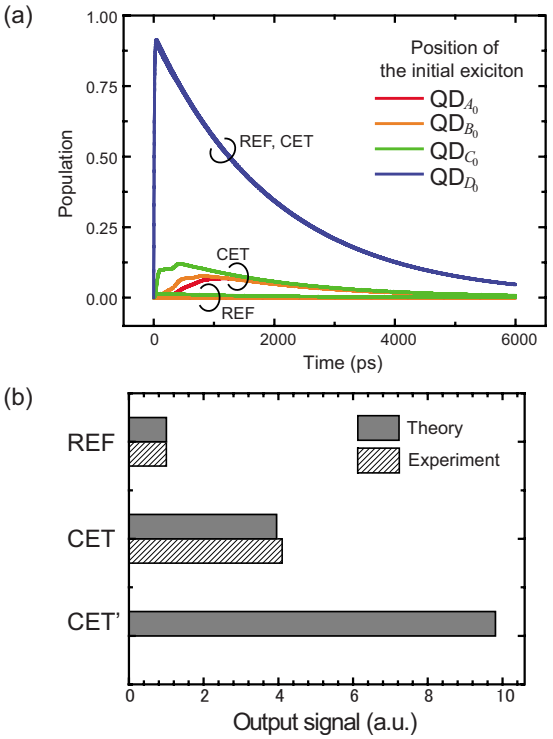

FIG. 3. (Color online) (a) Evolutions of the populations of the (1,0) level of QD_{D_0} from the REF and CET systems with their initial excitons in QD_{A_0}, QD_{B_0}, QD_{C_0}, or QD_{D_0}. (b) Comparison of the total output signal between the REF, CET, and CET' systems.

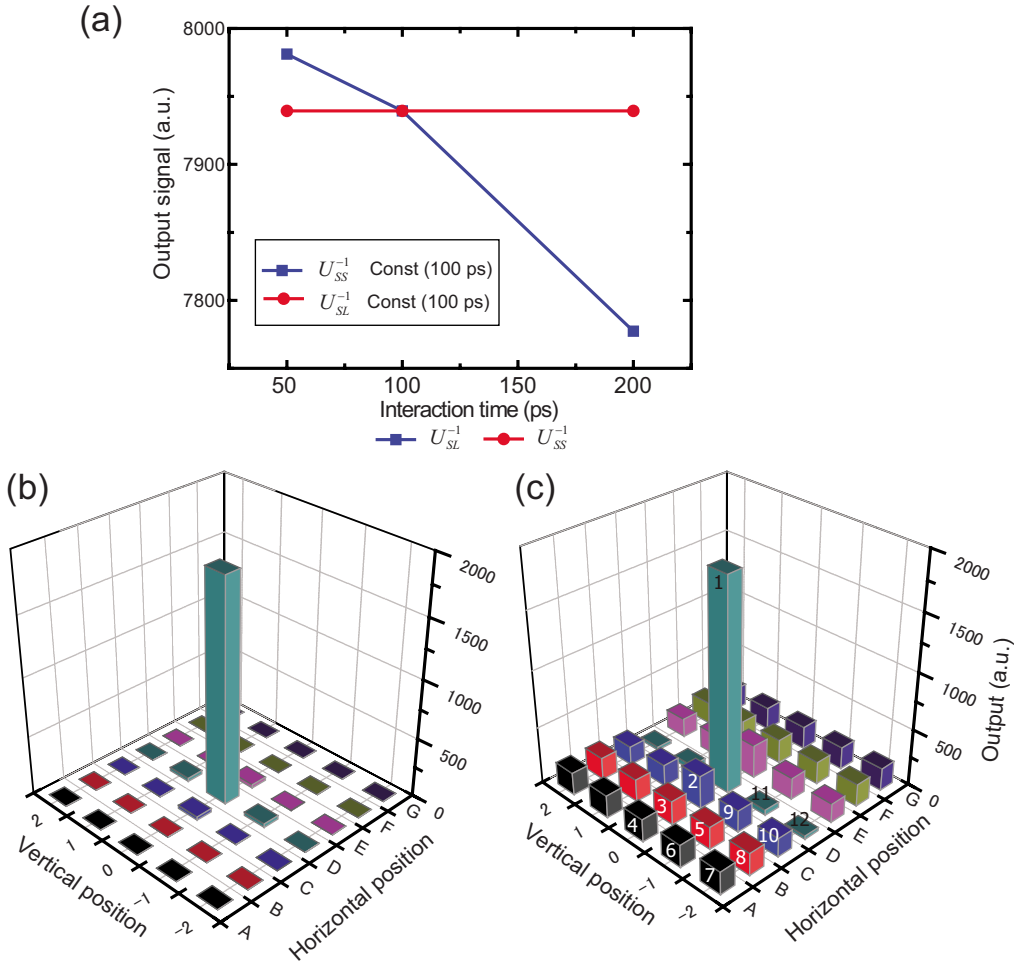

FIG. 4. (Color online) (a) Output signal dependency on the interdot horizontal and vertical near-field interactions. [(b) and (c)] Comparison of the output signal level as a function of initial position of the input exciton. The numbers attached to the bars in Fig. 4(c) indicate the order of the magnitude of the output signal.

onstrates $\rho_{D_0}(t;A_0)$, $\rho_{D_0}(t;B_0)$, and $\rho_{D_0}(t;C_0)$, all of which stay nearly at zero level. This is due to the fact that nearly all of the populations are trapped at the energy levels $A_0^{(1,0)}$, $B_0^{(1,0)}$, and $C_0^{(1,0)}$. The curve of $\rho_{D_0}(t;D_0)$ exhibits a higher population thanks to the sublevel relaxation from the (1,1) level to the (1,0) level in QD_{D_0}. The output signal for the initial excitation at S_i is obtained by integrating the time evolutions of $\rho_{D_0}(t;S_i)$ between 0 and 10 ns,

$$\gamma_{D_0}\int \rho_{D_0}(t;S_i)dt, \tag{7}$$

where $i=\{-2,\ldots,2\}$. The results are discussed and compared with those of the CET system in Figs. 3(b) and 4 in Sec. IV.

B. Analysis of the CET system

1. Modeling of the CET system

Next, with respect to the CET system, Fig. 2(b) represents a 5-row×7-column system composed of four kinds of quantum dots. The identification of each of the QDs is the same as with the REF system. Along the columns, the sizes of the quantum dots are uniform. The QDs located in the central column (column D) have the largest radius. The QDs located in their proximity, that is, in columns C and E, are smaller than those in column D and their radii are tuned such that, according to Eq. (1), the (1,0) levels of QD_{C_i} and QD_{E_i}, namely, $C_i^{(1,0)}$ and $E_i^{(1,0)}$, are resonant with those of the (1,1)-energy level of QD_{D_i}, that is, $D_i^{(1,1)}$. Similarly, we assume resonances between two levels in adjacent layers: $B_i^{(1,0)}=C_i^{(1,1)}=F_i^{(1,0)}=E_i^{(1,1)}$ and $A_i^{(1,0)}=B_i^{(1,1)}=G_i^{(1,0)}=F_i^{(1,1)}$.

Now, we formulate interdot interactions by introducing an interaction Hamiltonian. It is a block diagonal given by

$$H_{\mathrm{int}}=\begin{pmatrix} H_{AB} & O & O & O & O \\ O & H_{BC} & O & O & O \\ O & O & H_{CDE} & O & O \\ O & O & O & H_{EF} & O \\ O & O & O & O & H_{FG} \end{pmatrix}. \tag{8}$$

If state indices of H_{BC}, for example, are spanned by the order of $B_2^{(1,1)}$, $C_2^{(1,0)}$, $B_1^{(1,1)}$, $C_1^{(1,0)}$, $B_0^{(1,1)}$, $C_0^{(0,1)}$, $B_{-1}^{(1,1)}$, $C_{-1}^{(1,0)}$, $B_{-2}^{(1,1)}$, and $C_{-2}^{(1,0)}$, which are energetically degenerate, H_{BC} is given by

$$H_{BC} = \hbar \begin{pmatrix} 0 & U_{B_2C_2} & U_{B_1B_2} & 0 & 0 & 0 & 0 & 0 & 0 & 0 \\ U_{B_2C_2} & 0 & 0 & U_{C_1C_2} & 0 & 0 & 0 & 0 & 0 & 0 \\ U_{B_1B_2} & 0 & 0 & U_{B_1C_1} & U_{B_0B_1} & 0 & 0 & 0 & 0 & 0 \\ 0 & U_{C_1C_2} & U_{B_1C_1} & 0 & 0 & U_{C_0C_1} & 0 & 0 & 0 & 0 \\ 0 & 0 & U_{B_0B_1} & 0 & 0 & U_{B_0C_0} & U_{B_{-1}B_0} & 0 & 0 & 0 \\ 0 & 0 & 0 & U_{C_0C_1} & U_{B_0C_0} & 0 & 0 & U_{C_{-1}C_0} & 0 & 0 \\ 0 & 0 & 0 & 0 & U_{B_{-1}B_0} & 0 & 0 & U_{B_{-1}C_{-1}} & U_{B_{-2}B_{-1}} & 0 \\ 0 & 0 & 0 & 0 & 0 & U_{C_{-1}C_0} & U_{B_{-1}C_{-1}} & 0 & 0 & U_{C_{-2}C_{-1}} \\ 0 & 0 & 0 & 0 & 0 & 0 & U_{B_{-2}B_{-1}} & 0 & 0 & U_{B_{-2}C_{-2}} \\ 0 & 0 & 0 & 0 & 0 & 0 & 0 & U_{C_{-2}C_{-1}} & U_{B_{-2}C_{-2}} & 0 \end{pmatrix}, \tag{9}$$

where $U_{B_iC_i}$ represents the horizontal interactions between QD_{B_i} and QD_{C_i}, whereas $U_{C_iC_{i+1}}$ indicates vertical interactions between QD_{C_i} and $\mathrm{QD}_{C_{i+1}}$ through the energy level of $B_i^{(1,0)}(=C_i^{(1,1)})$. The relaxation constants for the corresponding states are given by

$$N_\Gamma^{BC} = \mathrm{diag}\left(\frac{\gamma_{B_2}}{2}, \frac{\Gamma_{C_2}}{2}, \frac{\gamma_{B_1}}{2}, \frac{\Gamma_{C_1}}{2}, \frac{\gamma_{B_0}}{2}, \frac{\Gamma_{C_0}}{2}, \frac{\gamma_{B_0}}{2}, \frac{\Gamma_{C_{-1}}}{2}, \frac{\gamma_{B_{-1}}}{2}, \frac{\Gamma_{C_{-2}}}{2}, \frac{\gamma_{B_{-2}}}{2} \right). \tag{10}$$

Letting $\rho_{BC}(t)$ be the density matrix for the above Hamiltonian, the master equation is given by

$$\frac{d\rho_{BC}(t)}{dt} = -\frac{i}{\hbar}[(H^{(0)} + H_{BC}), \rho_{BC}(t)] - N_\Gamma^{BC}\rho_{BC}(t) - \rho_{BC}(t)N_\Gamma^{BC} + P_\Gamma^{BC}[\rho_{AB}(t)]. \tag{11}$$

The last term on the right-hand side of Eq. (11) takes into account the fact that the lower level in QD_{B_i}, namely, the (1,0) level denoted by $B_i^{(1,0)}$, can be filled via the sublevel relaxation denoted by Γ_{B_i} from the upper level $B_i^{(1,1)}$, whose behavior is given by the differential equations that corresponds to Eq. (11) and whose density matrix is given by $\rho_{AB}(t)$.

2. Numerical evaluation of the CET system

In the numerical calculation, we first assume that the horizontal and vertical interactions are equal; namely, $U_{S_iT_i}^{-1} = U_{S_kS_{k+1}}^{-1} = 100$ ps. As in the REF system, the radiation lifetime of the bright QDs located in the center is $\gamma_{D_0}^{-1} = 2$ ns, and the sublevel relaxation time is $\Gamma_{S_i}^{-1} = 10$ ps. Again, we assume that only the relaxation from the (1,0) level in the center, that is, QD_{D_0}, contributes to the output. We assume that the system has an initial exciton in either the (1,1) level in $\mathrm{QD}_{S_i}(S = B, C, D, E, F)$ or the (1,0) level in $\mathrm{QD}_{S_i}(S = A, G)$.

IV. STRUCTURE-DEPENDENT EFFICIENCY OF OPTICAL EXCITATION TRANSFER

What is particularly notable in the CET system is that the excitons trapped in the trap states in columns *A*, *B*, *C*, *E*, *F*, and *G* have the chance to be transferred to the adjacent energy level through near-field interactions. Therefore, the probability of exciton transfer to the (1,0) level in D_0 from other dots could significantly improve. In fact, as shown in Fig. 3(a), $\rho_{D_0}(t;A_0)$, $\rho_{D_0}(t;B_0)$, and $\rho_{D_0}(t;C_0)$ in the CET system exhibit higher populations than in the REF system.

Finally, the output signal in the CET system is obtained by following the same procedure defined by Eq. (7), which is represented as the gray bar graph in Fig. 3(b); the enhancement factor with respect to the REF system is about 3.95, which agrees well with the experimental observations shown in Sec. II, indicated as the dashed bars in Fig. 3(b).

Figure 4(a) illustrates the dependency of the horizontal and vertical interdot interactions in the CET system. The circular marks in Fig. 4(a) show the output signal as a function of vertical interaction time $(U_{S_iS_{i+1}}^{-1})$ while the horizontal interactions remain constant $(U_{S_iT_i}^{-1} = 100$ ps). The output is nearly constant. On the other hand, the output increases as the horizontal interaction time $(U_{S_iT_i}^{-1})$ decreases keeping the vertical interactions constant $(U_{S_iS_{i+1}}^{-1} = 100$ ps), as shown by the square marks in Fig. 4(a). This clearly indicates that the energy transfers between the different-sized quantum dots via optical near-field interactions along the horizontal directions allow excitons to avoid being dissipated in trap states, leading to increased output signal.

Figures 4(b) and 4(c) summarizes the integrated output populations from QD_{D_0} as a function of the input excitation position for both the REF and CET systems. As is evident, the output populations from QD_{D_0} in the REF system are constituted almost entirely of an initial exciton located in QD_{D_0}, whereas in the CET system, the input excitons geometrically located far from QD_{D_0} can have an impact on the radiation from QD_{D_0}. Interestingly, regarding QDs in rows $i = -2$ and -1, distant QDs contribute to the output from

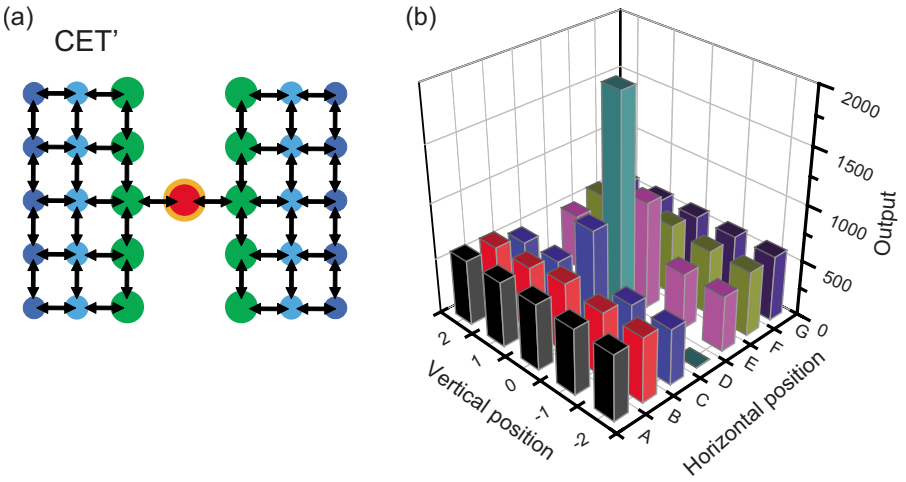

FIG. 5. (Color online) (a) Near-field interaction network in the CET' system where the nonradiative largest QDs are eliminated from the CET system. (b) The total excitation transfer in the CET' system is about 9.8 times larger than that in the REF system [see Fig. 3(b)].

QD_{D_0} more than the geometrically closer QDs do. For instance, QDs B_{-1} and B_{-2} contribute to the radiation from QD_{D_0} more than QDs such as C_{-1} and C_{-2} do. This is due to the fact that, for input excitons in QDs B_{-1} and B_{-2}, the chance of being trapped at QDs D_{-1} and D_{-2} is reduced.

Those internal mechanisms of optical excitation transfer in the CET system indicate that the output populations could be further improved by an appropriate design of the interaction network. For example, by removing the largest dark dots, namely, QDs D_{-2}, D_{-1}, D_1, and D_2, from the CET system, the output population should greatly improve because it eliminates the possibility of input excitons to be trapped at those QDs. Figure 5(a) schematically shows such a modified system denoted by CET'. As expected, the output populations from QD_{D_0} improved as shown in Fig. 5(b). As a total system, the output signal is about 9.8 times larger than that from the REF system.

V. CONCLUSION

We investigated the efficient optical excitation transfer in layered quantum dot structures by introducing a network of optical near-field interactions. With density-matrix-based modeling of the layered, graded-sized quantum dot systems, our theoretical analysis allows systematic handling of structure-dependent interdot interactions and reveals dominant factors contributing to the efficient optical excitation transfer. Our analysis shows good agreement with the experimental observations, where a graded-sized seven-layer QD system exhibits nearly four times larger photoluminescence compared with a uniform-sized QD system. We also show that the efficiency could be further improved by optimizing the interaction network.

We should also emphasize that the theoretical modeling strategy demonstrated in Sec. III can be applied to interaction networks other than the REF, CET, and CET' systems discussed in this paper. General properties that emerge from networks of optical near-field interactions on the nanometer-scale will be one important research challenge in the future. Experimentally, Akahane *et al.* realized stacked InAs QD devices consisting of more than 100 layers based on molecular-beam epitaxy.[16] Also, the sizes of QDs could potentially be controlled layer by layer. We will seek further theoretical and experimental insights in layered QD systems regarding their energy transfer efficiencies, as well as achieving functionalities for a wide range of system applications. Those pursuits will provide us with a further understanding of the network of optical near-field interactions in QD systems.

ACKNOWLEDGMENTS

This work was supported by the Japan Science and Technology Agency (JST) and the German Research Foundation (DFG) under the Strategic Japanese-German Cooperative Program. The authors acknowledge Thomas A. Klar of Ilmenau University of Technology for important suggestions. The authors acknowledge Christoph Lienau of the University of Oldenburg, the German-side principal investigator of the above Japan-Germany bilateral program, for fruitful discussions.

[1] M. Ohtsu, K. Kobayashi, T. Kawazoe, T. Yatsui, and M. Naruse, *Principles of Nanophotonics* (Taylor & Francis, Boca Raton, 2008).

[2] M. Ohtsu, K. Kobayashi, T. Kawazoe, S. Sangu, and T. Yatsui, IEEE J. Sel. Top. Quantum Electron. **8**, 839 (2002).

[3] M. Naruse, T. Miyazaki, F. Kubota, T. Kawazoe, K. Kobayashi, S. Sangu, and M. Ohtsu, Opt. Lett. **30**, 201 (2005).

[4] T. Unold, K. Mueller, C. Lienau, T. Elsaesser, and A. D. Wieck, Phys. Rev. Lett. **94**, 137404 (2005).

[5] P. Vasa, R. Pomraenke, S. Schwieger, Y. I. Mazur, V. Kunets, P. Srinivasan, E. Johnson, J. E. Kihm, D. S. Kim, E. Runge, G. Salamo, and C. Lienau, Phys. Rev. Lett. **101**, 116801 (2008).

[6] T. Kawazoe, K. Kobayashi, and M. Ohtsu, Appl. Phys. Lett. **86**, 103102 (2005).

[7] H. Tamura, J.-M. Mallet, M. Oheim, and I. Burghardt, J. Phys. Chem. C **113**, 7548 (2009).
[8] H. Imahori, J. Phys. Chem. B **108**, 6130 (2004).
[9] M. Kubo, Y. Mori, M. Otani, M. Murakami, Y. Ishibashi, M. Yasuda, K. Hosomizu, H. Miyasaka, H. Imahori, and S. Nakashima, J. Phys. Chem. A **111**, 5136 (2007).
[10] T. Kawazoe, K. Kobayashi, and M. Ohtsu, Appl. Phys. B **84**, 247 (2006).
[11] C. R. Kagan, C. B. Murray, M. Nirmal, and M. G. Bawendi, Phys. Rev. Lett. **76**, 1517 (1996).
[12] O. I. Mićić, K. M. Jones, A. Cahill, and A. J. Nozik, J. Phys. Chem. B **102**, 9791 (1998).
[13] S. V. Kershaw, M. T. Harrison, A. L. Rogach, and A. Kornowski, IEEE J. Sel. Top. Quantum Electron. **6**, 534 (2000).
[14] M. Naruse, T. Kawazoe, R. Ohta, W. Nomura, and M. Ohtsu, Phys. Rev. B **80**, 125325 (2009).
[15] S. A. Crooker, J. A. Hollingsworth, S. Tretiak, and V. I. Klimov, Phys. Rev. Lett. **89**, 186802 (2002).
[16] K. Akahane, N. Yamamoto, and M. Tsuchiya, Appl. Phys. Lett. **93**, 041121 (2008).
[17] T. Yatsui, S. Sangu, T. Kawazoe, M. Ohtsu, S. J. An, J. Yoo, and G.-C. Yi, Appl. Phys. Lett. **90**, 223110 (2007).
[18] T. Kawazoe, K. Kobayashi, J. Lim, Y. Narita, and M. Ohtsu, Phys. Rev. Lett. **88**, 067404 (2002).
[19] T. Franzl, T. A. Klar, S. Schietinger, A. L. Rogach, and J. Feldmann, Nano Lett. **4**, 1599 (2004).
[20] T. A. Klar, T. Franzl, A. L. Rogach, and J. Feldmann, Adv. Mater. **17**, 769 (2005).
[21] K. Nishibayashi, T. Kawazoe, K. Akahane, N. Yamamoto, and M. Ohtsu, Appl. Phys. Lett. **93**, 042101 (2008).
[22] T. Förster, Ann. Phys. **437**, 55 (1948).
[23] G. D. Scholes and G. R. Fleming, J. Phys. Chem. B **104**, 1854 (2000).
[24] M. Ohtsu, T. Kawazoe, T. Yatsui, and M. Naruse, IEEE J. Sel. Top. Quantum Electron. **14**, 1404 (2008).
[25] A. A. Mamedov, A. Belov, M. Giersig, N. N. Mamedova, and N. A. Kotov, J. Am. Chem. Soc. **123**, 7738 (2001).
[26] T. Franzl, D. S. Koktysh, T. A. Klar, A. L. Rogach, J. Feldmann, and N. Gaponik, Appl. Phys. Lett. **84**, 2904 (2004).
[27] A. L. Rogach, T. Franzl, T. A. Klar, J. Feldmann, N. Gaponik, V. Lesnyak, A. Shavel, A. Eychmüller, Y. P. Rakovich, and J. F. Donegan, J. Phys. Chem. C **111**, 14628 (2007).
[28] L. E. Brus, J. Chem. Phys. **80**, 4403 (1984).
[29] H. Haug and S. W. Koch, *Quantum Theory of the Optical and Electronic Properties of Semiconductors* (World Scientific, Singapore, 2004).
[30] A. L. Rogach, L. Katsikas, A. Kornowski, D. Su, A. Eychmüller, and H. Weller, Ber. Bunsenges. Phys. Chem. **100**, 1772 (1996).
[31] S. Sangu, K. Kobayashi, A. Shojiguchi, T. Kawazoe, and M. Ohtsu, J. Appl. Phys. **93**, 2937 (2003).
[32] H. J. Carmichael, *Statistical Methods in Quantum Optics 1* (Springer-Verlag, Berlin, 1999).
[33] A. M. Kapitonov, A. P. Stupak, S. V. Gaponenko, E. P. Petrov, A. L. Rogach, and A. J. Eychmüller, J. Phys. Chem. B **103**, 10109 (1999).
[34] S. Mayilo, J. Hilhorst, A. S. Susha, C. Hhl, T. Franzl, T. A. Klar, A. L. Rogach, and J. Feldmann, J. Phys. Chem. C **112**, 14589 (2008).